



Fuzzy control of backside weld width in cold metal transfer welding of X65 pipeline in the vertical-up position

Zhijiang Wang^{1,2} · Zhendong Chen^{1,2} · Shaojie Wu^{1,2} · Caiyan Deng^{1,2} · Zhichen Lin^{1,2}

Received: 15 August 2023 / Accepted: 27 November 2023 / Published online: 5 December 2023
© International Institute of Welding 2023

Abstract

Reasonable backside weld geometry of the root-pass welding is the basic guarantee for good fatigue performance of the weld joints. In the vertical-up (3G) position welding, the change in the force direction on the molten pool makes the degree of penetration reduced, such that a small disturbance in the welding process will lead to uneven weld geometry and discontinuous weld penetration states. In order to obtain a good weld penetration state for root pass by cold metal transfer (CMT) welding in the vertical-up position, a control strategy applicable to CMT root-pass welding was proposed. The backside weld width (W_b) is related to the welding heat input (q) and the peak current time ratio (PTR). As per that base current almost does not affect the long period, and the long period tends to disappear in the range with small peak current or wire feed speed, a welding program with a stable PTR was designed, and the W_b prediction model was simplified to be only related to q . Based on the simplified model, a fuzzy controller was designed and its control effects for W_b in the CMT root-pass welding were tested. The test results proved the validity of the control strategy under normal fit-up conditions and the condition with varying misalignments.

Keywords Heat input · Peak current time ratio · Backside weld width · Fuzzy control · Vertical-up (3G) position · CMT root-pass welding

Nomenclature

e Error between \hat{q} and q^* in the control system, J/mm
 E Fuzzy variable for e
 ec The change in error, J/(mm·s)
 EC Fuzzy variable for ec
 I Welding current, A
 \hat{I} Welding current data by Hall sensor, A
 I_b Welding current in base current stage, A
 I_p Welding current in peak current stage, A
 I_{sc} Welding current in short-circuiting current stage, A
 LPR Long period ratio, i.e., the ratio of the number for long periods over the number for all periods, %

n Total number of periods (or cycles) in the calculation
 PTR Peak current time ratio, i.e., the average ratio of peak current time over the welding time, %
 q Welding heat input, J/mm
 \hat{q} Output of the control system, J/mm
 q^* Reference (or expected output) of the control system, J/mm
 q_b Heat input for a base current stage, J/mm
 q_i Heat input in period i , J/mm
 q_p Heat input for a peak current stage, J/mm
 q_{sc} Heat input for a short-circuiting current stage, J/mm
 t Time, s
 t_b Base current time, ms
 t_p Peak current time, ms
 t_{sc} Short-circuiting current time, ms
 U Arc voltage, V
 \hat{U} Arc voltage data by Hall sensor, V
 U_b Arc voltage in base current stage, V
 U_p Arc voltage in peak current stage, V
 U_{sc} Arc voltage in short-circuiting current stage, V

Recommended for publication by Commission XII - Arc Welding Processes and Production Systems

✉ Zhijiang Wang
wangzj@tju.edu.cn

¹ Tianjin Key Laboratory of Advanced Joining Technology, Tianjin 150004, China

² School of Materials Science and Engineering, Tianjin University, Tianjin 150004, China

uc	The input of control system, i.e., the increment of v_f , m/min
UC	Fuzzy variable for uc
v	Welding speed, m/min
v_f	Wire feed speed, m/min
W_b	Backside weld width, mm
W_b^*	Expected backside weld width, mm

1 Introduction

When laying of the large-diameter and thick-wall steel pipes, the efficiency and quality of manual welding cannot meet the fabrication requirements; thus, mechanized welding is employed. Due to lack of real-time monitoring of the pipe welding process, it is easy to produce discontinuous penetration, unreasonable backside weld geometry, and other issues. Under the complex welding conditions, it is not enough to guarantee the backside weld geometry only by optimizing welding parameters. Therefore, the closed-loop control of it is particularly important. In the vertical-up (3G) position welding, the gravity of the weld pool no longer promotes the penetration, and the degree of penetration is usually reduced, compared with that in the flat (1G) position. Minor changes in welding conditions may cause discontinuous penetration. Therefore, it is necessary to control the backside weld geometry in the vertical-up position.

Cold metal transfer (CMT) welding technology has been widely used in the root-pass welding of pipes due to its advantages, such as low heat input, no spatter, good weld formation, and strong bridging ability [1–3], but there is little research on the penetration control of CMT. This is because the CMT waveform is complex, which is designed for spatter elimination and stable droplet transfer; the penetration control should not deteriorate the droplet transfer process, and the coupling of welding parameters in the MIG/MAG synergic welding mode greatly increases the difficulty in its control. In addition, the change in welding position leads to the instability of CMT welding process. Kim et al. [4] studied the backside weld geometry of the CMT root-pass welding without backing, which found that the full penetration cannot be obtained when the groove angle is small and the gap is 0. With the increase in groove angle, the weld achieved full penetration with a gap of 2–6 mm, and the backside weld was well shaped [4]. Recently, the relationship between welding heat input (q), peak current time ratio (PTR), and backside weld width (W_b) in the CMT root-pass welding of pipes in the vertical-up position was studied in our previous study [5]. Therefore, the main objective of this work is to find a closed-loop control strategy applicable to the MIG/MAG synergic welding mode and to realize real-time control of the backside weld geometry in the vertical-up welding position based on the established prediction model.

After obtaining a series of information, such as arc sound, light, and electricity, which can characterize the weld geometry through sensing technology, the characteristic signals need to be processed with some rules to keep them near the expected value, so as to achieve the real-time control of the weld geometry. Different processing rules for characteristic signals correspond to different control algorithms. The proportional-integral-derivative (PID) control is a classical control method, which is the most widely used one in practical engineering. Fan et al. [6] established the relationship between weld pool geometry parameters and W_b based on the three-optical-path vision sensor in the gas tungsten arc welding (GTAW) process and used a PID controller to control W_b by controlling the weld pool width. PID control is more suitable for a single input single output (SISO) linear time-invariant system, but the welding process is usually a multiple input multiple output (MIMO) nonlinear time-variant dynamic process; therefore, modern control methods, such as adaptive control and predictive control, were applied in the weld geometry control. Chen et al. [7] identified the linear time-variant process model for the pulsed GTAW online, using the minimum variance strategy, and realized the real-time control of W_b by adjusting the peak current. Wang et al. [8] employed the interval model to improve robustness of the adaptive predictive controller for the penetration depth control in the pulsed gas metal arc welding (GMAW-P). Zou et al. [9] applied a Hammerstein model to adaptively control of the GMAW-P weld penetration depth based on the relative fluctuation coefficient of the weld pool. Cao et al. [10] identified a MIMO linear model to describe the GMAW-P welding process, established a prediction model based on the state-space method, and designed a double input double output adaptive predictive controller based on this prediction model to control W_b in real time.

Traditional control methods usually require accurate mathematical models based on the control plant, but some complex control processes, such as welding, are with uncertain or cannot be described by traditional mathematical models, for which the intelligent control, such as fuzzy control, neural network control [11, 12], expert system control [13], was proposed to handle the uncertainty. Fuzzy control is a relatively mature one. Chen et al. [14] predicted W_b by using the topside weld pool geometry and welding parameters and controlled W_b in the 1G position welding by a fuzzy controller. Tsai et al. [15] collected the backside weld pool width in real time and took it as the feedback for the weld penetration. And a fuzzy controller was designed to adjust the welding current to control the weld penetration. Gao et al. [16] predicted W_b based on welding current, gap, and weld width and designed a fuzzy controller to control W_b in real time in the butt-joint fabrication by GTAW.

The foregoing researches were mainly applicable to the 1G position. In the researches for other positions, Wang

et al. [17] established a prediction model of W_b by neural network and realized the penetration control in GTAW-P in the horizontal position by stepping welding. Li et al. [18, 19] established a predictive controller to control the weld penetration in the all-position (5G) welding by indirectly controlling the arc voltage. In addition, weld geometry control in the welding process with the short-circuiting transfer is less studied. In the present work, CMT root-pass welding process of pipe in the vertical-up position will be investigated, in which a control strategy applicable to the MIG/MAG synergic welding mode is designed to control W_b in real time based on the simplification of the prediction model of W_b in our previous study [5].

2 Experimental design

2.1 Control strategy analysis

As per our previous study, W_b is related to q and PTR , and the relationship between the three is as follows [5]:

$$W_b = -120.9 - 2.917 \times PTR + 0.752 \times q + 7.333 \times 10^{-3} \times PTR \times q - 1.111 \times 10^{-3} \times q^2 \quad (1)$$

in which

$$PTR = t_p / (t_p + t_b + t_{sc}) \quad (2)$$

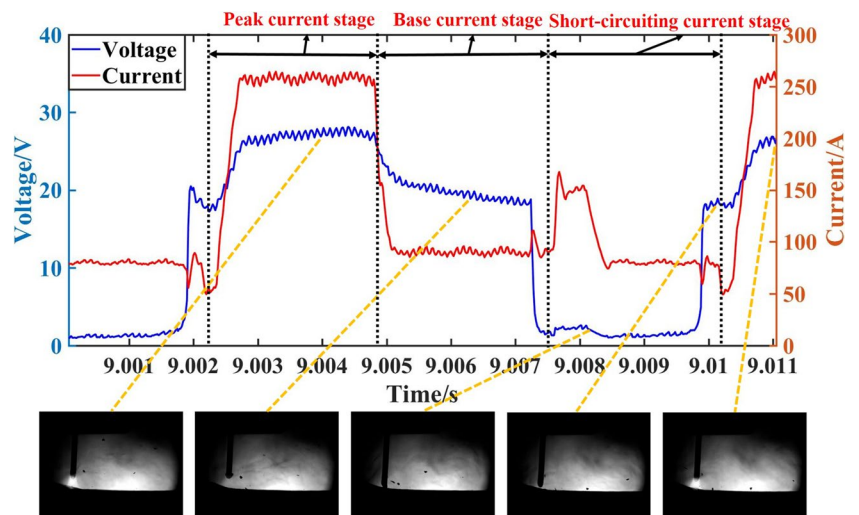
where t_p means peak current time, t_b means base current time, and t_{sc} means short-circuiting current time, as shown in Fig. 1, which shows that a typical CMT period (or cycle) can be divided into three stages, i.e., peak current stage, base current stage, and short-circuiting current stage [5], and

$$q = \frac{\sum q_i}{n} = \frac{1}{n} \sum \frac{q_p \times t_p + q_b \times t_b + q_{sc} \times t_{sc}}{t_p + t_b + t_{sc}} \quad (3)$$

where q_i means the heat input in period i ; q_p is the heat input for a peak current stage and $q_p = \frac{U_p \times I_p}{v}$; q_b is the heat input for a base current stage and $q_b = \frac{U_b \times I_b}{v}$; q_{sc} is the heat input for a short-circuiting current stage and $q_{sc} = \frac{U_{sc} \times I_{sc}}{v}$; and n represents the total number of periods (or cycles) in the calculation. Note: U_p , U_b , and U_{sc} are for the arc voltage in peak current stage, in base current stage and in short-circuiting current stage, respectively; I_p , I_b , and I_{sc} are for the welding current in peak current stage, in base current stage, and in short-circuiting current stage, respectively; and v is for the welding speed.

Equation 1 shows that W_b can be regulated by controlling the characteristic signals q and PTR . However, W_b is related to both q and PTR , and when the welding parameters, such as I_p and wire feed speed (v_f), are adjusted, q and PTR will both change, resulting in a complex relationship between welding parameters and characteristic signals and a difficulty to establish an effective control strategy. Therefore, the prediction model needs to be simplified. Since all welding parameters will affect q , it is a good choice to find a way to minimize the influences of PTR on W_b such that only q needs to be controlled in the control system. Figure 2 is the block diagram of the W_b control system. q is the output of the control plant (i.e., welding process or arc), which has a determined relationship with the controlled variable W_b . \hat{q} is the feedback, which is calculated by the real-time welding current (\hat{I}) and voltage (\hat{U}) data acquired from the welding process by the Hall sensors for welding current (I) and voltage (U). And q^* is the reference (or the expected output) of the welding process. \hat{q} is compared with q^* , and the difference between the two, e , is used as the input of the

Fig. 1 CMT welding process [5], including the typical current and voltage signal and droplet transfer process



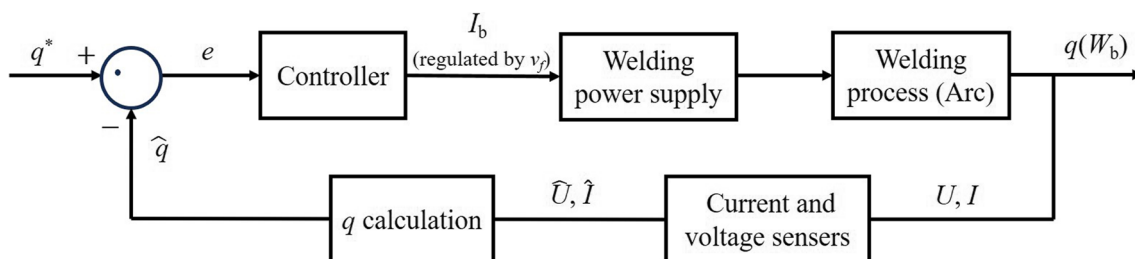


Fig. 2 Block diagram of the W_b control system

controller. The controller outputs the change in controlled variable, namely I_b that was also recommended by ref. [5] and is regulated by v_f to regulate welding process and further to affect q in the welding process.

2.2 Experimental equipment and materials

Based on the established prediction model, an appropriate control algorithm was used to conduct the control test. Since the standard MIG/MAG welding mode does not support real-time adjustment of welding parameters in the welding process, the MIG/MAG synergic welding mode was employed for control tests. The experimental setup is shown in Fig. 3. The whole system is divided into two parts, namely welding system and control system. The welding system includes a welding power supply, CMT Advanced

4000, with a wire feeder, VR 7000 CMT. The control system includes Moeller U-C123E Hall current and voltage sensors, NI PCI-6221 acquisition card, BNC-2120 connection card, and CMT ROB5000 control interface. The current and voltage signals were collected in real-time, and the collection frequency was 5000 Hz. The electrical signals are input to the computer via the PCI-6221 acquisition card, and the characteristic signal is calculated by an algorithm in the controller to represent the weld penetration. After processing by the controller, the control signal, which is determined by the control algorithm, is then output via the PCI-6221 card and is sent to ROB5000 control interface. The ROB5000 control interface communicates with the CMT power supply to adjust welding parameters in real time.

The material used was API 5L X65 pipeline steel with a diameter of 355.0 mm and a thickness of 13.5 mm, and

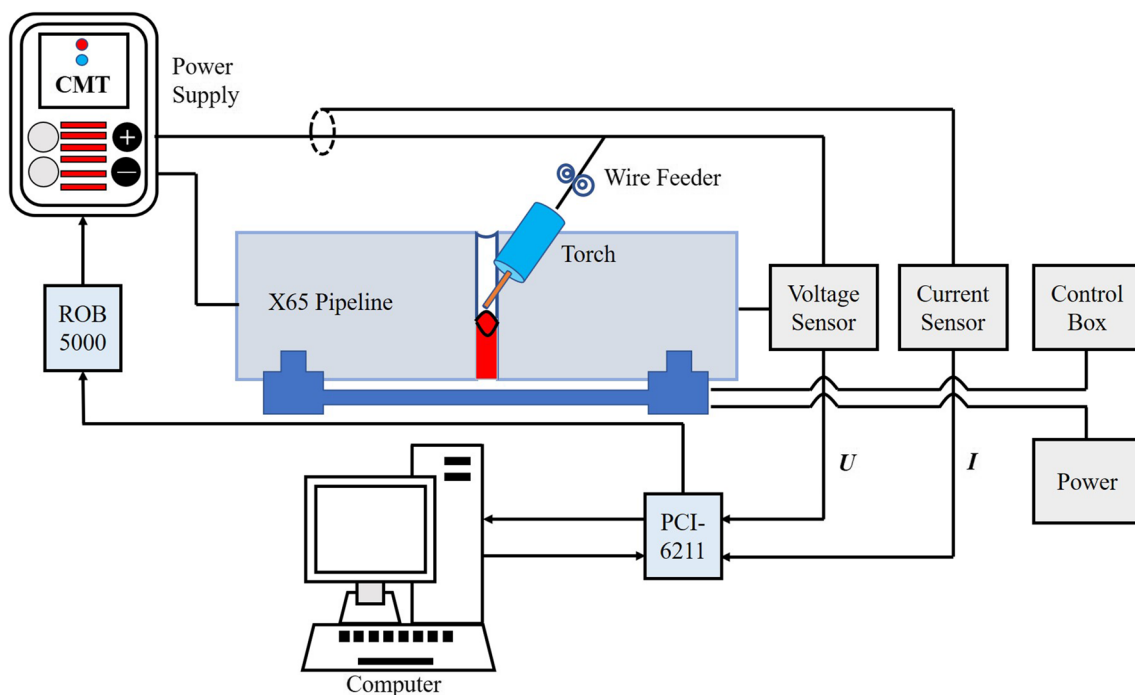


Fig. 3 Vertical-up welding control system

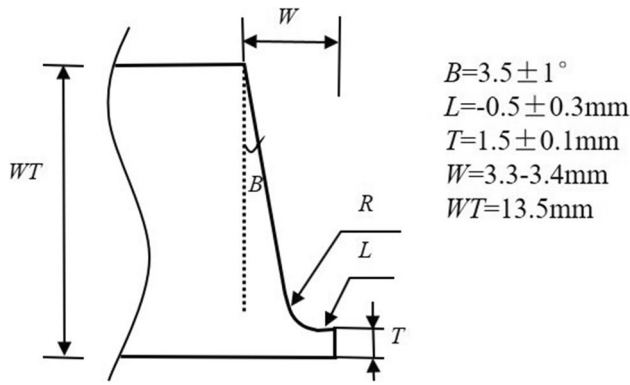


Fig. 4 Schematic diagram of the “U” groove

a “U”-shaped groove without gap was used, as shown in Fig. 4. ER70S-6 welding wire with a diameter of 1.2 mm was used as filler material. Table 1 shows the chemical composition of the X65 pipeline steel and welding wire. A mixture gas of 80%Ar + 20%CO₂ was used as shielding gas, and the gas flow rate was 15–20 L/min.

2.3 Welding program setting

In the conditions of the 3G welding position or increasing I_p in the CMT welding process, “the long period” will occur [5]. “The long period” is defined as the period when the base current time (t_b) is greater than 5 ms in the present work.

As per the foregoing discussion in Sect. 2.1, to simplify the model, a good choice is to keep one parameter, i.e., PRT , unchanged during the control process. From ref. [5], I_b has little influence on PTR , PTR is basically kept at approximately 25%, and I_b is positively correlated with q . Therefore,

I_b was selected as the control variable. In the MIG/MAG synergic welding mode, other welding parameters can only be adjusted by adjusting v_f , but v_f affects both q and PTR . Figure 5 shows the long period ratio (LPR), which is the ratio of the number for long periods over the number for all periods, with different welding parameters. From Fig. 5a, as v_f decreases, LPR decreases. When v_f was set to a small value, the long period tended to disappear and the droplet transfer process tended to be stable. Therefore, keeping v_f within a range of small values can make its influence on q and PTR tend to disappear. A change in I_p causes both q and PTR (Fig. 5b) to change. Therefore, I_p was set as a fixed value. Based on the foregoing discussion, the CMT welding program can be customized in such a way that a v_f only corresponds to a welding curve, whose parameters are the same as other welding curves except I_b ; and v_f is set within a range with small values to eliminate its influence on q and PTR . In this way, v_f is adjusted only to regulate I_b , and only I_b has influence on characteristic signals, i.e., q . Thus, the model is simplified, in which W_b is controlled only by controlling q .

From Fig. 5b, LPR tends to zero when I_p is small. When the I_p was 260 A, the LPR was only 6.67%, while a large LPR would make the welding process unstable, resulting in defects, such as discontinuous weld penetration. Therefore, when customizing the welding curve, I_p , I_{sc} , and t_p were as 260 A, 80 A, and 2.5 ms, respectively, to ensure the stable droplet transfer process. Herein, the maximum v_f was set as 5 m/min, and the minimum v_f was 3.0 m/min. The maximum I_b was set as 140 A, and the minimum I_b was 40 A. A v_f was customized to an I_b , whose relationship is listed in Table 2. After welding curve customization, the CMT power supply can adjust welding parameters in real time via ROB5000 control interface.

Table 1 Chemical composition of API 5L X65 and welding wire (wt%)

	C	Mn	Si	S	P	Fe
API 5L X65	0.050	1.400	0.220	0.050	0.040	Balance
ER70S-6	0.073	1.490	0.880	0.011	0.010	Balance

Fig. 5 Relationship between welding parameters and LPR . a v_f ; b I_p

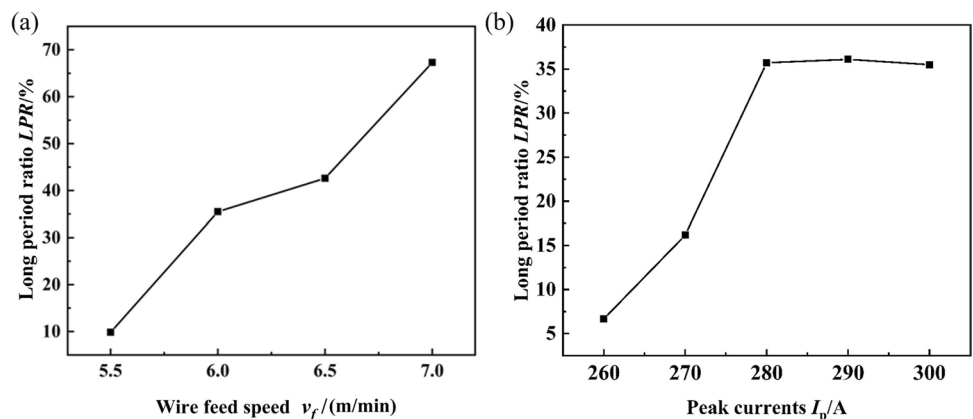


Table 2 The relationship between v_f and I_b

v_f /(m/min)	I_b /A	v_f /(m/min)	I_b /A
3.0	40	4.1	95
3.1	45	4.2	100
3.2	50	4.3	105
3.3	55	4.4	110
3.4	60	4.5	115
3.5	65	4.6	120
3.6	70	4.7	125
3.7	75	4.8	130
3.8	80	4.9	135
3.9	85	5.0	140
4.0	90		

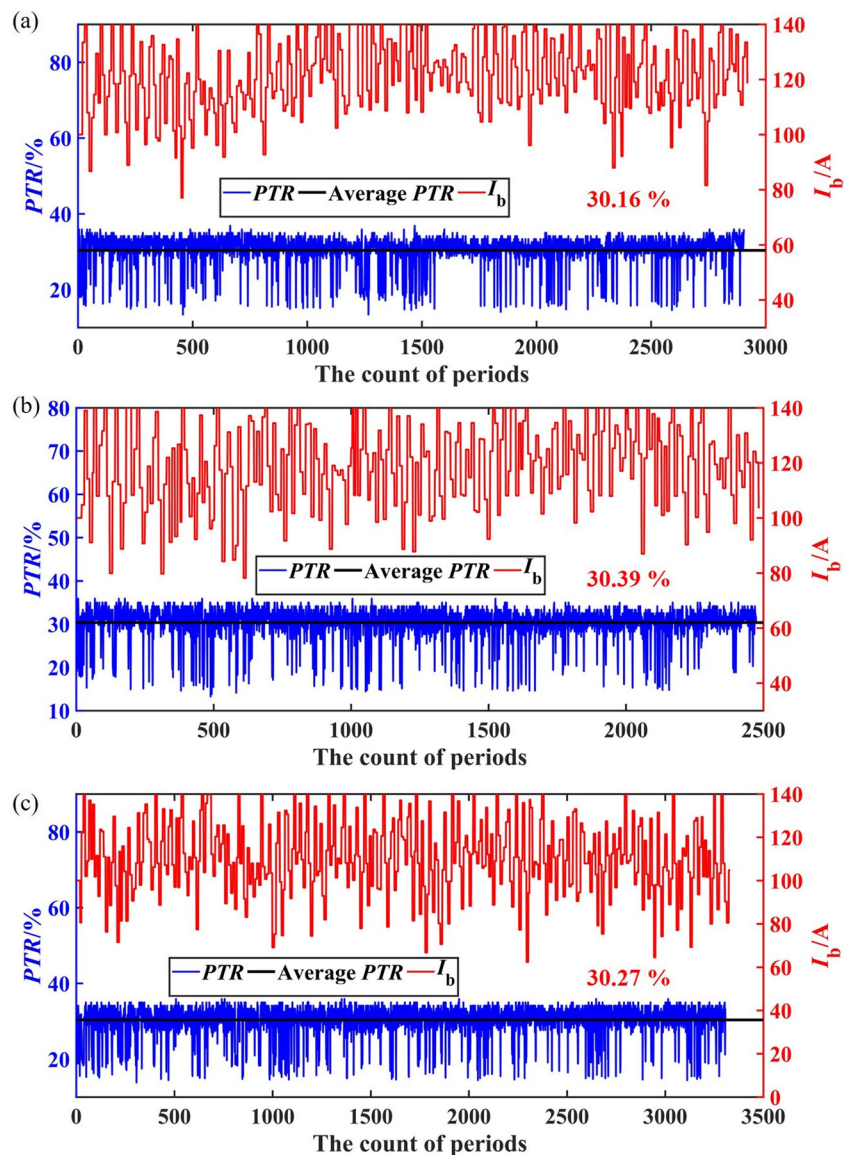
In order to make sure that the PTR does not change under this welding program, three groups of tests were conducted with randomly v_f signals (i.e., regulated I_b). Figure 6 shows the input signals and the calculated PTR . PTR s in all three groups were kept at approximately 30.00%, which further indicated that changing I_b has little influence on PTR . When PTR is 30.00%, i.e., taking $PTR=30\%$ into Eq. 1, the relationship between q and W_b is shown in Fig. 7 and Eq. 4. W_b was then controlled according to this relationship in subsequent tests.

$$W_b = -0.001111 \times q^2 + 0.972 \times q - 208.41 \quad (\text{when } PTR = 30\%) \quad (4)$$

2.4 Fuzzy controller design

Fuzzy controller generates control rules as per human experience and achieves ideal control effect by fuzzy logic

Fig. 6 Calculated PTR when v_f signals were randomly input. **a** Test 1, **b** test 2, **c** test 3



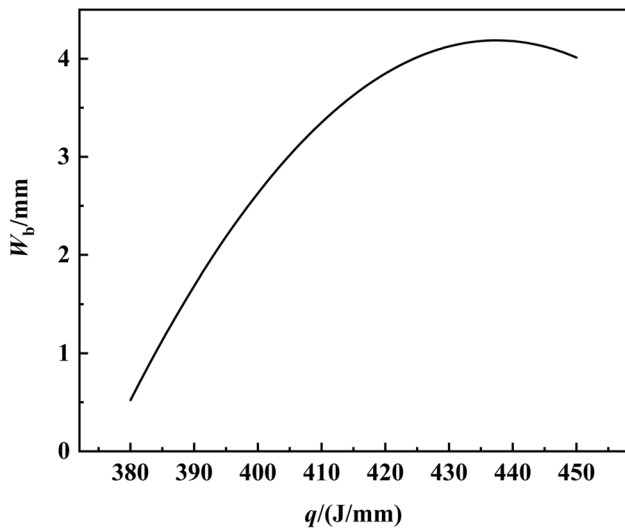


Fig. 7 The relationship between q and W_b when PTR is 30.00%

reasoning. The biggest difference between fuzzy control and traditional control is that it does not need a mathematical model. Due to the complex influences of CMT welding parameters on q , and t_b and t_{sc} are not constants and change randomly with the droplet transfer process, it is difficult to establish an accurate mathematical model, and the discreteness of I_b in the customized welding program also makes mathematical modeling difficult. Therefore, fuzzy control was selected to control W_b in real time in the present work.

According to the simplified model, W_b can be characterized only by q when PTR is unchanged. Therefore, \hat{q} was employed as feedback, and I_b , i.e., the output of the controller, was adjusted by regulating v_f in real time by fuzzy controller to control W_b .

Since there is no piecewise linear relationship between the CMT welding parameters and q , Mamdani type was selected as the fuzzy controller. Single input will make the fuzzy rules simple and thus reduce the precision of the control system. The multiple input and single output (MISO) control system has a complex structure and long fuzzy reasoning time. Therefore, Mamdani fuzzy controller with

the structure of double input and single output (DISO) was employed.

The real-time calculated feedback is the average welding heat input in the CMT welding process within three periods, represented by \hat{q} ; the expected system output is q^* ; e is the difference between \hat{q} and q^* ; ec is the difference between two neighbored \hat{q} ; and uc is the increment of v_f . At instant t :

$$e = \hat{q} - q^* \tag{5}$$

$$ec = e(t) - e(t - 1) = \hat{q}(t) - \hat{q}(t - 1) \tag{6}$$

Figure 8 shows the processing flow of the fuzzy controller. e and ec are used as the input of the fuzzy controller. The fuzzy variables corresponding to e and ec are E and EC , respectively. After e and ec are input into the fuzzy controller, the two variables are fuzzified, and then, fuzzy reasoning is conducted according to the fuzzy rules, after which a fuzzy variable UC can be obtained; uc is the output of fuzzy controller, which is the defuzzification results of UC .

Seven linguistic terms, i.e., PB, PM, PS, ZO, NS, NM, and NB, are selected to describe the fuzzy variables. The fuzzy subsets of E , EC , and UC are all {PB, PM, PS, ZO, NS, NM, NB}. As per the preliminary experiments, the range of input and output variables was defined respectively. The ranges of e , ec , and uc are $[-100, 100]$, $[-50, 50]$, and $[-1, 1]$, respectively. After fuzzification, the ranges of E , EC , and UC are all $[-6, 6]$.

The fuzzy subsets of each fuzzy variable are described by membership function, as shown in Fig. 9. Except that ZO for E is with a membership function of trapezoidal, NS, ZO, and PS for E , EC , and UC are with triangular ones, while NB, NM, PM, and PB are with Gaussian ones. In the CMT welding process, when the difference between \hat{q} and q^* is small, if the fuzzy controller adjusts the welding parameters at this time, it is easy to cause overshooting, since I_b is discrete in the customized CMT welding program and steps every 5 A. Therefore, the membership function of ZO for E was set as a trapezoid function. The membership function of NS, ZO,

Fig. 8 Processing flow of the fuzzy controller

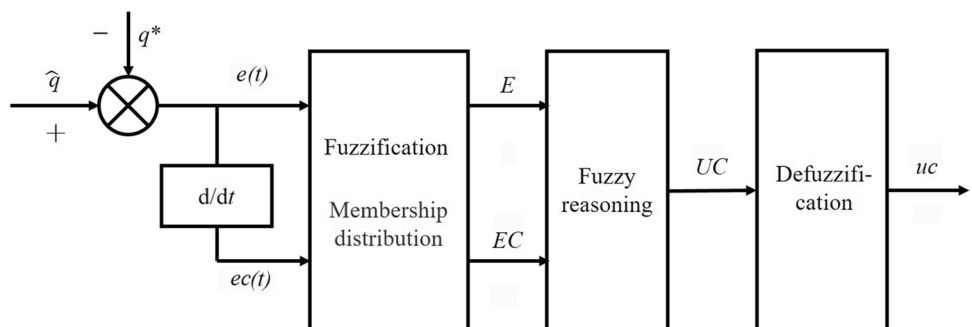
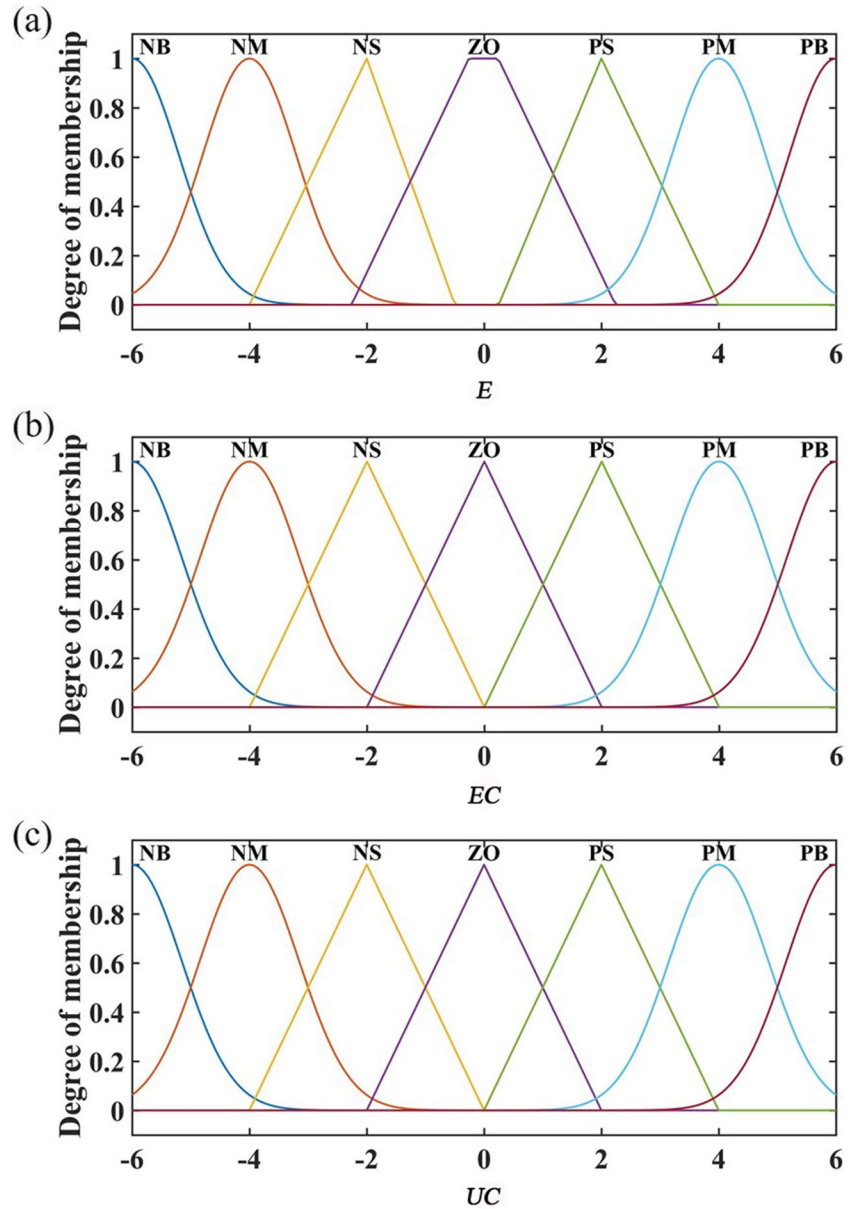


Fig. 9 Membership function distribution. **a** E ; **b** EC ; **c** UC



and PS was set as triangle function because triangle function has a high precision and is applicable when the difference between \hat{q} and q^* is small.

As per the preliminary experiments, fuzzy rules were formulated with reference to the following rules. When \hat{q} is greater than q^* (e is positive) and \hat{q} for the current instant is greater than \hat{q} for the previous instant (ec is positive), v_f should be decreased, that is, decrease I_b ; when e and ec are both negative, increase I_b ; when plus-minus sign for e and ec are opposite, I_b is adjusted according to the influences of the two on \hat{q} in the next cycle; when e and ec both fluctuate around 0, the welding parameters are kept unchanged.

Table 3 lists 49 fuzzy control rules. In fuzzy reasoning, the “Max–Min” compositional rule of inference method was used. Defuzzification is the process of converting fuzzy variable UC into precise variable uc , that is, sharpening of fuzzy variable. The centroid method was used to do the defuzzification. Figure 10 illustrates the fuzzy rules.

A PID controller was also designed to compare with fuzzy controller. The performance comparisons were done in a simulation environment. The input and output of the PID controller are e and I_b , respectively. The main parameters for the PID controller are as follows: $K_P=0.25$; $K_I=0.015$; $K_D=0.012$.

Table 3 Fuzzy rules

	<i>UC</i>	<i>E</i>						
		NB	NM	NS	ZO	PS	PM	PB
<i>EC</i>	NB	PB	PB	PM	PM	PS	PS	ZO
	NM	PB	PM	PM	PS	PS	ZO	NS
	NS	PM	PM	PS	PS	ZO	NS	NS
	ZO	PM	PS	PS	ZO	NS	NS	NM
	PS	PS	PS	ZO	NS	NS	NM	NM
	PM	PS	ZO	NS	NS	NM	NM	NB
	PB	ZO	NS	NS	NM	NM	NB	NB

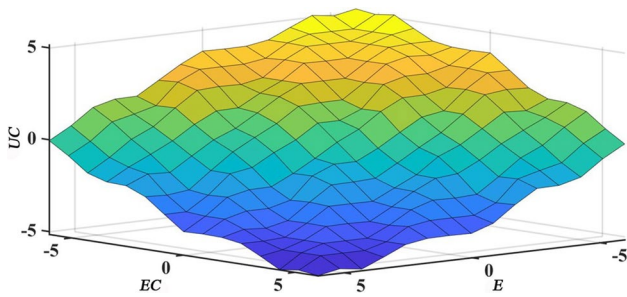


Fig. 10 Illustration of fuzzy rules

3 Experimental results and discussion

3.1 Open-loop control test

Open-loop control test was conducted using the customized welding program mentioned above. v_f was kept at 4.2 m/min during welding, that is, I_b was set to 100 A. Figure 11 shows the open-loop control test results. From Fig. 11a, W_b gradually decreased from the start to the end, and the backside weld geometry was uneven. This is because the cross section of the pipe is not a regular circle, the change in the contact tip to work distance (*CTWD*) will lead to the change in arc length, and arc length is positively correlated with arc voltage. From Fig. 11b, the average arc voltage gradually decreased, indicating that *CTWD* gradually decreased, while the average current was basically unchanged. The decrease in the average arc voltage will lead to the decrease in q , as shown in Fig. 11c, resulting in a gradual decrease in W_b . The test results showed that closed-loop control is necessary to obtain stable backside weld geometry under complex and varying welding conditions.

3.2 Performance comparisons between fuzzy and PID controller

In the simulations of the two controllers, two references, i.e., $q^* = 560$ J/mm and $q^* = 580$ J/mm, were selected, which results are shown in Fig. 12. From Fig. 12, fuzzy control performs a little bit better in dynamic response; and it has a better accuracy, since the discreteness of I_b (5 A in a step) in the customized welding program makes the PID controller fluctuate around the references with an amplitude that is larger than fuzzy control. Therefore, the performance of fuzzy controller is better and it is selected as the controller to conduct the following welding tests.

3.3 Fuzzy control test with a fixed set point

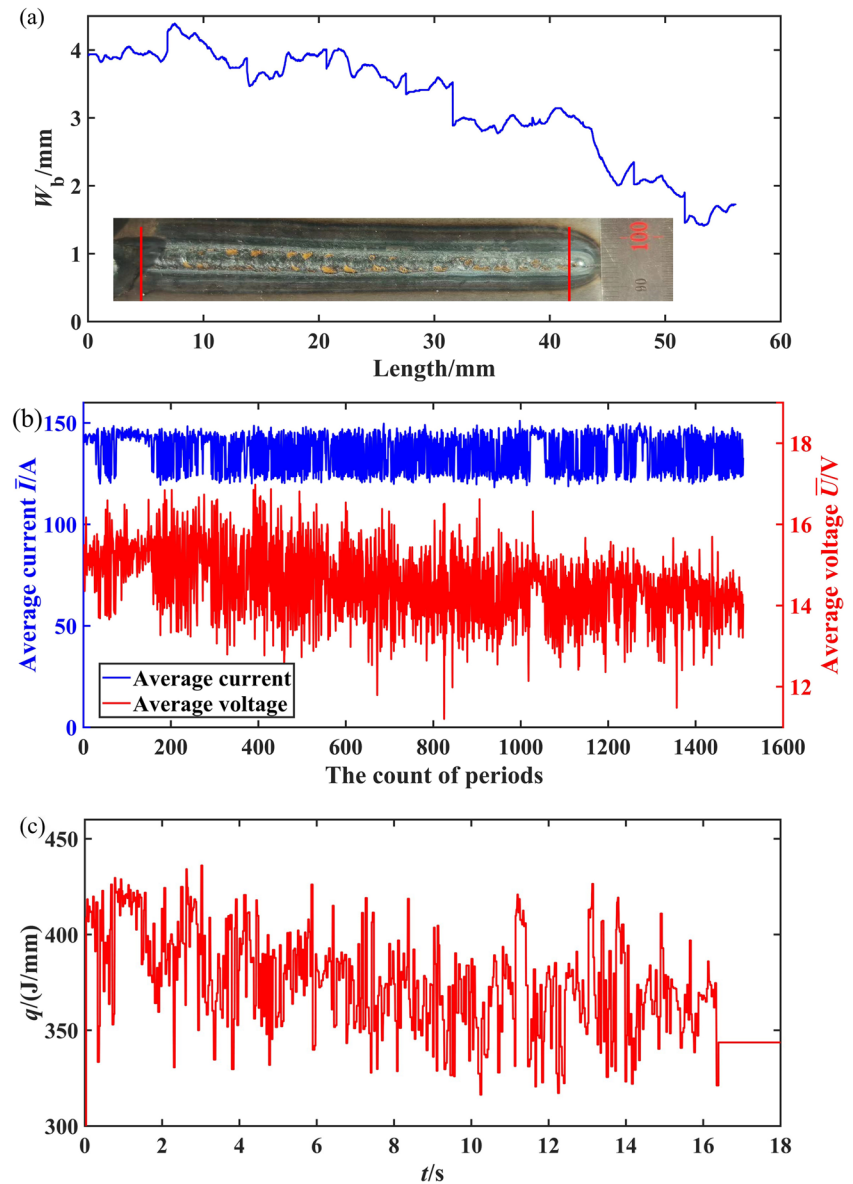
To verify the closed-loop control effect with a fixed set point for the fuzzy controller, a control test was conducted, in which the calculated \hat{q} is controlled around an expected value to keep the same degree of penetration during welding. When an expected W_b , i.e., W_b^* , is set, q^* can be calculated as per Eq. 4. During the execution of the closed-loop control, the controller will adjust the system input I_b according to the difference between the \hat{q} and q^* and the changes in \hat{q} , so that the system output fluctuates around the expected one.

Figure 13 shows the fuzzy control test results with a fixed set point. W_b^* was set as 4.15 mm, that is, q^* was 432 J/mm. From Fig. 13a, with the closed-loop control, the backside weld geometry was relatively uniform, and the measured W_b also fluctuated around the expected one. From Fig. 13b, the output of the system was fluctuating around the expected one. When the output of system deviated from the expected value, the controller could adjust the input of system (I_b) quickly and effectively according to the fuzzy rules illustrated in Fig. 10.

3.4 Fuzzy control test with varying misalignments

In order to further verify the applicability and robustness of the fuzzy controller for W_b , a fuzzy control test with varying misalignments was designed. Figure 14 shows the schematic

Fig. 11 Backside weld geometry and electric signals under open-loop control test. **a** Backside weld geometry; **b** average current and voltage; **c** q



of the pipe with varying misalignments. The misalignments at points d and f are the largest, i.e., 1 mm, and those at points a and e are the smallest, i.e., 0 mm.

A fuzzy control test with a fixed set point was conducted under the condition of varying misalignments. In the test, the corresponding part of the pipes with varying misalignments was placed at the 3 o'clock position. The welding start point was point b, and the end point was point c, as marked in in Fig. 14. Accordingly, the range of misalignments was 0.49–0.86 mm. \hat{q} was controlled to fluctuate around q^* in the test, as shown in Fig. 15b. When q^* was set to 416 J/mm, W_b^* was 3.70 mm. The actual measurement results showed that W_b fluctuated around the expected one, as shown in Fig. 15a. The test results showed that the simplified W_b prediction

model and fuzzy controller established in the present work can be applicable in the condition of varying misalignments.

3.5 Fuzzy control test with varying gap

The pipe used in the test with varying gap has the maximum gap at point d (1.0 mm) and the minimum gap at point a (0 mm), as shown in Fig. 16.

The varying gap results in significant changes in heat dissipation conditions, which makes the prediction model established in the present work ineffective. q^* should be reduced to prevent burn through. In the fuzzy control test with varying gap, q^* was set as 336 J/mm; the corresponding gap was placed at the 3 o'clock

Fig. 12 Simulation results for PID and fuzzy controllers. **a** $q^* = 560$ J/mm; **b** $q^* = 580$ J/mm

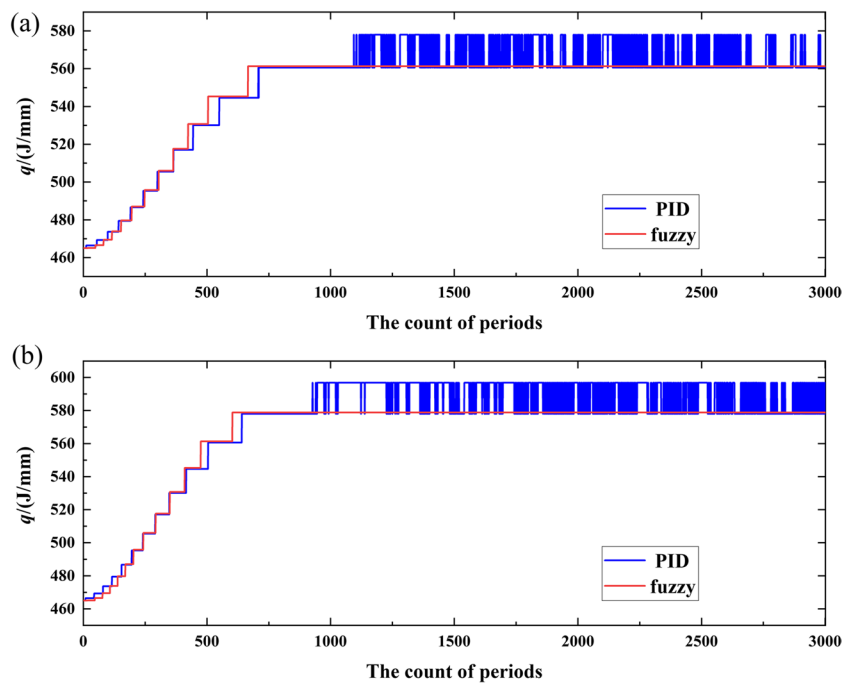
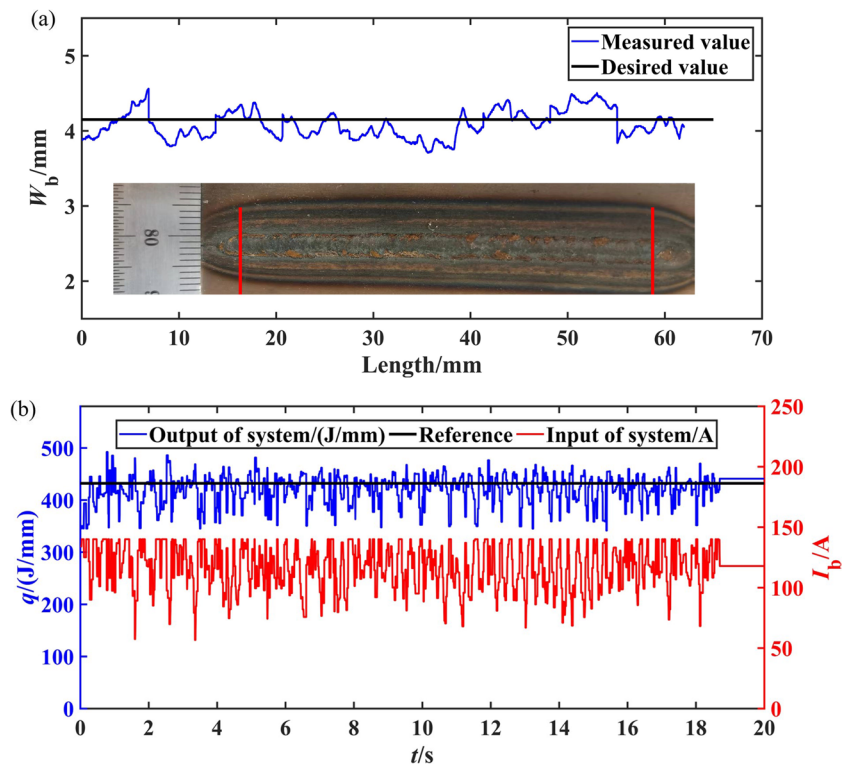


Fig. 13 Backside weld geometry, and input and output of the control system in the fuzzy control test with a fixed set point of 432 J/mm. **a** The backside weld geometry; **b** the input and output of the control system



position. The welding start point of the test was point b, and the end point was point c, as marked in Fig. 16. Accordingly, the gap range was 0.25–0.50 mm. The test results are shown in Fig. 17. As the gap gradually increased, W_b gradually increased with the same q , as shown in Fig. 17a. From Fig. 17b, the fuzzy control

system could still work effectively, and the output of system \hat{q} was controlled to fluctuate around the set point q^* , but W_b changed. In order to solve the issue that the simplified W_b prediction model loses efficacy due to significant changes in heat dissipation under the condition of varying gap, the gap size should be

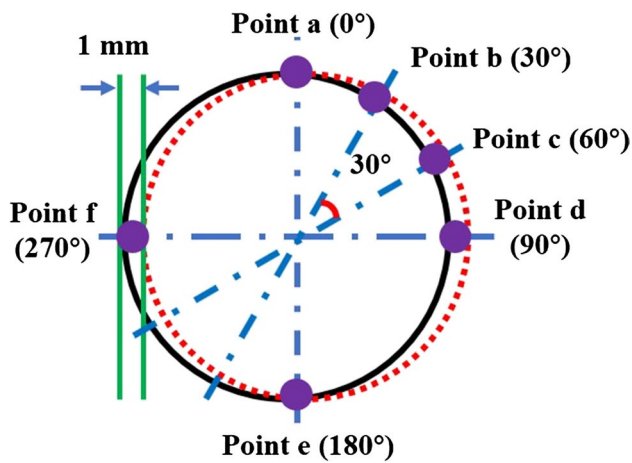


Fig. 14 Schematic of varying misalignments of the pipe

introduced into the prediction model, and the feed-forward control should be added in the controller, in which the gap should be measured in real time, and q^* should be adjusted accordingly as per the gap size, with the expectation of making W_b uniform and stable.

4 Conclusions and future work

The prediction model of W_b in the vertical-up position of the pipe by the CMT welding with the proposed U groove was simplified; a closed-loop control method applicable to the MIG/MAG synergic welding mode was explored in the CMT welding process; and its effectiveness was verified in the actual welding tests. The main conclusions are as follows:

Fig. 15 Fuzzy control test under the condition of varying misalignments. **a** The backside weld geometry; **b** the input and output of the control system when the set point was 416 J/mm and the misalignment range was 0.49–0.86 mm

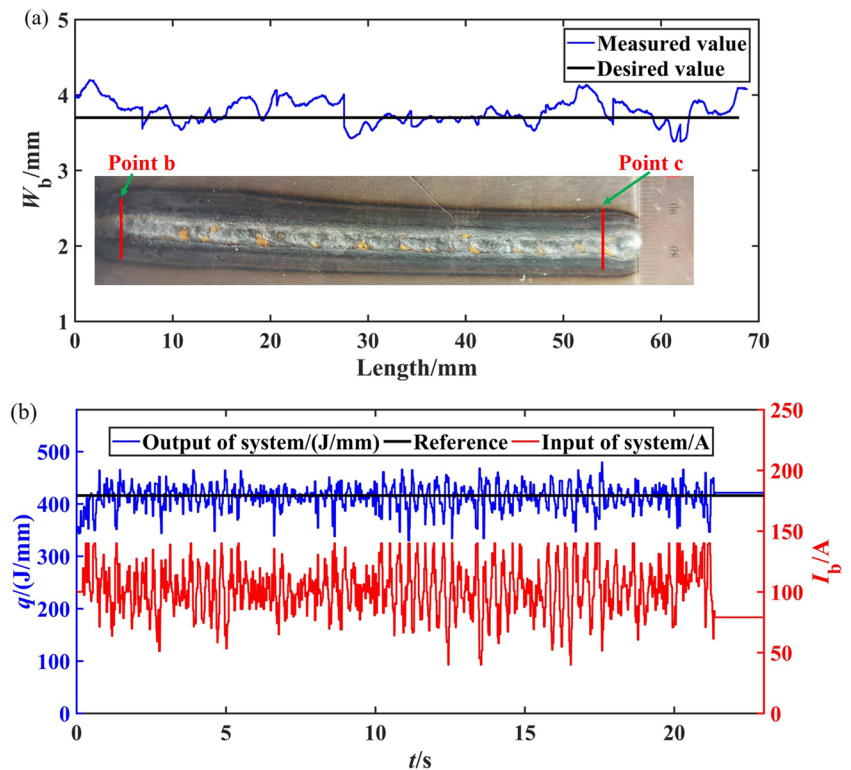


Fig. 16 Schematic of the varying gap of pipe (illustration with the pipe being cut into two halves)

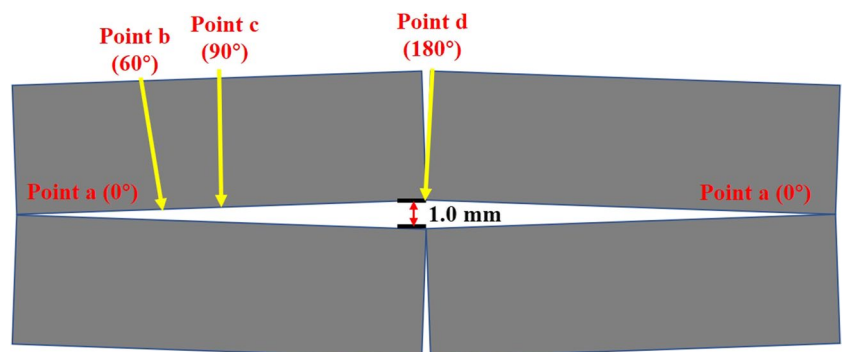
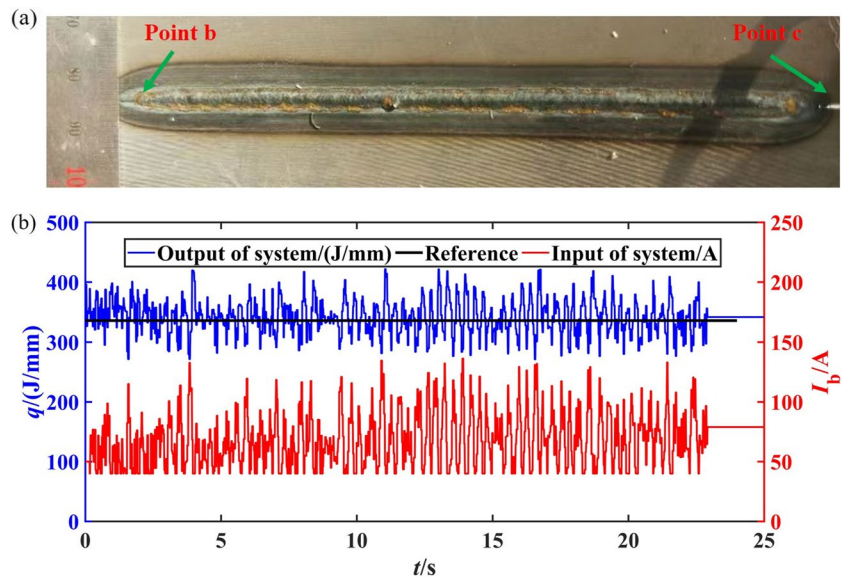


Fig. 17 Fuzzy control test under the condition of varying gap. **a** The backside weld geometry; **b** the input and output of the control system when the set point was 332 J/mm and the gap range was 0.25–0.50 mm



1) With consideration of the characteristics of the MIG/MAG synergic welding mode, which adjusts v_f to adjust other welding parameters, the welding program was customized. I_p and v_f has little influence on PTR when they are small; thus, I_p was kept at a fixed low value of 260 A, and v_f was set within a range of small values, i.e., 3.0–5.0 m/min, to ensure that PTR remained unchanged in the welding program. Keeping other parameters unchanged in the welding curves corresponding to each v_f , the change in v_f is ensured to only affect I_b . Accordingly, the prediction model of W_b was simplified so that it is only related to q . When PTR is 30.00%, the simplified prediction model of W_b in the vertical-up position by the CMT welding with the proposed U groove is as follows:

$$W_b = -0.001111 \times q^2 + 0.972 \times q - 208.41$$

2) The fuzzy controller was designed with the fuzzy reasoning rules, which were formulated as per the preliminary experiments. When e and ec are both positive, decrease I_b ; when e and ec are both negative, increase I_b ; when the plus-minus sign for e and ec are opposite, I_b is adjusted according to the influences of the two on \hat{q} in the next cycle; when e and ec both fluctuate around 0, the welding parameters are kept unchanged.

3) The fuzzy control system for W_b in the vertical-up position by the CMT welding was tested and verified. The fuzzy control tests under normal conditions and under the condition of varying misalignment showed that the controller can control the output of system q near the

expected value by adjusting the input of system I_b , so as to obtain the expected W_b .

However, in the condition of varying gap, due to significant changes in heat dissipation, the simplified prediction model of W_b lost efficacy, so it is necessary to introduce independent variable, gap size, into the prediction model of W_b for improvement. This work will be conducted in the future.

Author contribution Zhijiang Wang: conceptualization, methodology, formal analysis, resources, writing (review and editing), funding acquisition, project administration.

Zhendong Chen: methodology, software, formal analysis, investigation, data curation, visualization, writing—original draft.

Shaojie Wu: formal analysis, validation, writing—review and editing.

Caiyan Deng: formal analysis, validation, supervision.

Zhichen Lin: software, formal analysis, data curation, writing—review and editing.

Funding This study is supported by the National Natural Science Foundation of China (Grant No.: 52375374).

Data availability The datasets generated during and/or analyzed during the current study are available from the corresponding author on reasonable request.

Code availability The codes are not publicly available due to the commercial restriction.

Declarations

Ethics approval Not applicable.

Consent to participate Not applicable.

Consent for publication The authors give their consent for the publication of identifiable details, which can include photograph(s) and/or videos and/or case history and/or details within the text to be published in *Welding in the World*.

Conflict of interest The authors declare no competing interests.

References

- Kumar NP, Devarajan PK, Vendan SA et al (2017) Prediction of bead geometry in cold metal transfer welding using back propagation neural network. *Int J Adv Manuf Technol* 93:385–392
- Nandan G, Kumar G, Arora KS et al (2022) MIG and CMT brazing of aluminum alloys and steel: a review. *Mater Today: Process* 56(1):481–488
- Selvi S, Vishvakshnan A, Rajasekar E (2018) Cold metal transfer (CMT) technology – an overview. *Def Technol* 14(1):28–44
- Kim JS, Lee JP, Park MH et al (2014) A study on prediction of the optimal process parameters for GMA root-pass welding in pipeline. *Procedia Eng* 97:723–731
- Chen ZD, Wang ZJ, Wang FR et al (2023) Feasibility study on sensing and prediction of backside weld geometry in cold metal transfer welding of X65 pipeline in vertical-up position. *J Manuf Processes* 85:1173–1186
- Fan CJ, Lv FL, Chen SB (2009) Visual sensing and penetration control in aluminum alloy pulsed GTA welding. *Int J Adv Manuf Technol* 42(1–2):126–137
- Chen H, Lv F, Lin T et al (2009) Closed-loop control of robotic arc welding system with full-penetration monitoring. *J Intell Robot Syst* 56(5):565–578
- Wang ZJ, Zhang YM, Wu L (2012) Adaptive interval model control of weld pool surface in pulsed gas metal arc welding. *Automatica* 48(1):233–238
- Zou SY, Wang ZJ, Hu SS et al (2020) Control of weld penetration depth using relative fluctuation coefficient as feedback. *J Intell Manuf* 31:1203–1213
- Cao Y, Wang ZJ, Hu SS et al (2021) Modeling of weld penetration control system in GMAW-P using NARMAX methods. *J Manuf Process* 65:512–524
- Lv N, Xu YL, Li SC et al (2017) Automated control of welding penetration based on audio sensing technology. *J Mater Process Technol* 250:81–89
- Aviles-Vias JF, Rios-Cabrera R, Lopez-Juarez I (2016) On-line learning of welding bead geometry in industrial robots. *Int J Adv Manuf Technol* 83(1):217–231
- Lou YJ (1998) Intelligent control for pulsed GTAW dynamic process based on image sensing of weld pool. Dissertation, Harbin Institute of Technology (in Chinese)
- Chen SB, Lou YJ, Wu L et al (2000) Intelligent methodology for sensing, modeling and control of pulsed GTAW: part 1 - bead-on-plate welding. *Weld J* 79(6):151s–163s
- Tsai CH, Hou KH, Chuang HT (2006) Fuzzy control of pulse GTA welds by using real-time root bead image feedback. *J Mater Process Technol* 176(1–3):158–167
- Gao XD, Huang SS, Yu YL (2000) Fuzzy neural networks for control of penetration depth during GTAW. *China Weld* 9(1):1–8
- Wang ZJ, Zeng ZT, Wu SJ et al (2023) Weld penetration control of wire-filled pulsed gas tungsten arc welding of pipe in the horizontal position. *Weld World* 67:1793–1807
- Li XR, Shao Z, Zhang YM et al (2013) Monitoring and control of penetration in GTAW and pipe welding. *Weld J* 92:190s–196s
- Li XR, Zhang YM (2014) Predictive control for manual plasma arc pipe welding. *J Manuf Sci Eng* 136(4):041017

Publisher's Note Springer Nature remains neutral with regard to jurisdictional claims in published maps and institutional affiliations.

Springer Nature or its licensor (e.g. a society or other partner) holds exclusive rights to this article under a publishing agreement with the author(s) or other rightsholder(s); author self-archiving of the accepted manuscript version of this article is solely governed by the terms of such publishing agreement and applicable law.